



Published in final edited form as:

Clin Cancer Res. 2017 July 01; 23(13): 3371–3384. doi:10.1158/1078-0432.CCR-16-2142.

PI3K Inhibition Reduces Mammary Tumor Growth and Facilitates Anti-tumor Immunity and Anti-PD1 Responses

Jiqing Sai^{1,2,*}, Philip Owens^{1,2,*}, Sergey V. Novitskiy³, Oriana E. Hawkins^{1,2}, Anna E. Vilgelm^{1,2}, Jinming Yang^{1,2}, Tammy Sobolik^{1,2}, Nicole Lavender^{1,2}, Andrew C. Johnson^{1,2}, Colt McClain^{4,§}, Gregory D. Ayers⁵, Mark C. Kelley⁶, Melinda Sanders⁴, Ingrid A. Mayer³, Harold L. Moses², Mark Boothby⁴, and Ann Richmond^{1,2,#}

¹Tennessee Valley Healthcare System, Department of Veterans Affairs, Nashville, TN

²Department of Cancer Biology, Vanderbilt University, Nashville, TN

³Department of Medicine, Vanderbilt University, Nashville, TN

⁴Department of Pathology, Microbiology and Immunology, Vanderbilt University, Nashville, TN

⁵Department of Biostatistics, Vanderbilt University, Nashville, TN

⁶Department of Surgical Oncology, Vanderbilt University, Nashville, TN

Abstract

Purpose—Metastatic breast cancers continue to elude current therapeutic strategies, including those utilizing PI3K inhibitors. Given the prominent role of PI3K α,β in tumor growth and PI3K γ,δ in immune cell function, we sought to determine whether PI3K inhibition altered anti-tumor immunity.

Experimental Design—The effect of PI3K inhibition on tumor growth, metastasis, and anti-tumor immune response was characterized in mouse models utilizing orthotopic implants of 4T1 or PyMT mammary tumors into syngeneic or PI3K γ null mice, and patient-derived breast cancer xenografts in humanized mice. Tumor infiltrating leukocytes were characterized by IHC and FACS

#Corresponding author: Dr. Ann Richmond, Ph. D., Dept. of Cancer Biology, 432 Preston Research Building, 2220 Pierce Avenue, Vanderbilt University Medical Center, Nashville, TN 37232, Tel.: 615-343-7777, Fax: 615-936-4687, ann.richmond@vanderbilt.edu.

*These two authors contributed equally to the work described in this paper

OEH, Current address: ENTVantage DX, Fort Worth TX

§CM, Current address: Saint Thomas Hospital, Nashville, TN.

The authors have no conflicts of interest to disclose

*Additional methodology can be found in the Supplement.

Author Contributions:

Conception and design: A. Richmond, J Sai, P Owens, S Novitskiy, OE Hawkins, M. Boothby, H.L.Moses

Development of methodology: J Sai, P Owens, S Novitskiy, OE Hawkins, J Yang.

Acquisition of data: (provided animals, acquired and managed patients, provided facilities, etc): J Sai, P Owens, S Novitskiy, OE Hawkins, AE Vilgelm, J Yang, M Kelley, C. Andrew Johnson, T Sobolik, N. Lavender, C McClain, M Sanders, I A Mayer

Analysis and Interpretation of data (e.g., statistical analysis, biostatistics, computational analysis): GD Ayers, J Yang, J Sai, P Owens, S Novitskiy, OE Hawkins, T. Sobolik, C McClain, M Sanders, I A Mayer.

Writing, review and/or revision of the manuscript: A Richmond, J Sai,, P Owens, S Novitskiy, OE Hawkins, AE Vilgelm, M Boothby, M Sanders, HL Moses

Administrative, technical, or material support: CA Johnson

Study supervision: A Richmond

Other (tissue acquisition of human tumor xenografts, clinical information): MC Kelley, M Sanders

analysis in BKM120 (30mg/kg, QD) or vehicle treated mice and PI3K γ^{null} versus PI3K γ^{WT} mice. Based on the finding that PI3K inhibition resulted in a more inflammatory tumor leukocyte infiltrate, the therapeutic efficacy of BKM120 (30mg/kg, QD) and anti-PD1 (100 μ g, twice weekly) was evaluated in PyMT tumor bearing mice.

Results—Our findings show that PI3K activity facilitates tumor growth and surprisingly, restrains tumor immune surveillance. These activities could be partially suppressed by BKM120 or by genetic deletion of PI3K γ in the host. The anti-tumor effect of PI3K γ loss in host, but not tumor, was partially reversed by CD8+T cell depletion. Treatment with therapeutic doses of both BKM120 and antibody to PD-1 resulted in consistent inhibition of tumor growth compared to either agent alone.

Conclusions—PI3K inhibition slows tumor growth, enhances anti-tumor immunity, and heightens susceptibility to immune checkpoint inhibitors. We propose that combining PI3K inhibition with anti-PD1 may be a viable therapeutic approach for triple negative breast cancer.

Introduction

One of every eight women in America will develop breast cancer in her life and in the US alone we have over 40,000 annual deaths due to this disease [1]. Breast cancers often arise due to somatic genetic mutations [2], and mutations that result in activation of pathways related to phosphoinositide 3-kinase (PI3K) are common in these tumors. PI3Ks form an evolutionarily conserved family of lipid kinases whose members include Class I A catalytic subunits (p110 α , β , δ); a Class 1B catalytic subunit (p110 γ); Class I regulatory domains (p85 α , β , γ , p150, p101, p87); Class II subunits (C2 α , C2 β , C2 γ); and a Class 3 protein (Vps34). The Class IA PI3K known as PIK3CA (p110 α) plays a critical role in a wide range of carcinomas and one third of somatic gene mutations in breast cancer patient tumors occur in this kinase family [2].

Several reports have shown that breast cancer patients with activating PIK3CA mutation have a poor prognosis [3, 4]. In contrast, patients with estrogen receptor or progesterone receptor positive tumors with PIK3CA mutation have a better long term survival [5–10]. Several PI3K inhibitors are in clinical trials for many cancers and early results point to multiple mechanisms by which breast tumors do not respond or develop resistance to PI3K inhibitors [11, 12]. As a result PI3K inhibitors are being evaluated in clinical trials in combination with AKT inhibitors, CDK4/6 inhibitors, MTOR inhibitors, HER2 inhibitors, MEK inhibitors, aromatase inhibitors, enzalutamide, tamoxifen, cisplatin, and paclitaxel, but often at the expense of considerable added toxicity [13–16]. GDC-0941 (potent inhibitor of PI3K α/δ (IC₅₀ 3nM) with some activity for β and γ isoforms (IC₅₀ 33 and 75nM)) from Genentech is in phase II clinical trials [17] [18] in combination with endocrine therapy, paclitaxel/docetaxel; BLY719, a selective PI3K α inhibitor from Novartis (IC₅₀ of 5nM) in combination with the CDK4/6 inhibitor LEE011 is in phase 1b/II trials in ER+ HER2-metastatic breast cancer. The Novartis compound BKM120 inhibits α , δ , β , and γ with IC₅₀'s of 52, 116, 166 and 262 nM, respectively. It is currently in clinical trials [19] and it has been examined in ER+ or HER2+ breast cancer, alone and in combination with a variety of other inhibitors [14, 20].

PI3K activities within cancer cells are important for tumor cell growth, proliferation, survival, motility and metastasis; they also play vital roles in leukocyte recruitment and activation, maintenance of vascular integrity and other aspects of the tumor microenvironment (TME) [21]. These features underscore the crucial need to determine the interplay between cancer cell-intrinsic functions of PI3K and anti-tumor immune responses. Stromal tumor infiltrating lymphocytes (TILs) may be an indicator for better prognosis for triple negative breast cancer [22]. One concern in using pan PI3K inhibitors is that PI3K δ and γ are important for leukocyte activation and migration, respectively [23, 24]. For this reason, studies were launched using δ - and γ -sparing PI3K inhibitors.

One strategy used by transformed cells to evade immune surveillance is to activate immune checkpoints, the immune inhibitory signals that normally restrict immune cell over-activation. Exciting evidence shows that immune-evading strategies utilized by some tumor cells can be targeted with antibodies that block checkpoint inhibition [25–27]. Alternatively, immune cells can be manipulated *ex vivo* and then infused back into cancer patients to provide enhanced anti-tumor activity [28] [29]. However, many cancers, including breast cancers, are often refractory to these interventions. Use of immunotherapy such as PD-1 blockade monotherapy has only been successful in a small percent of breast cancer patients, thus new combinations are being sought to combine existing targeted and immune based therapies [30].

In the study described herein, we evaluated the effects of pan-PI3K inhibition with BKM120 on anti-tumor immunity. We also determined whether combining BKM120 with PD-1 checkpoint inhibitor blockade would be advantageous for breast cancers. We show here that when host PI3K activity, both intrinsic and extrinsic to the cancer cells, is inhibited, the net effect is reduction of growth and metastasis of mammary adenocarcinomas. Systemic inhibition of PI3K with BKM120 effectively inhibited MMTV-PyMT and 4T1 tumor growth and/or metastasis in an orthotopic and syngeneic mammary tumor allograft model. Breast tumor PDX were also inhibited in immune deficient mouse models and in humanized immune competent mouse models. Moreover, the simple loss of PI3K γ alone in host cells, but not tumor cells, resulted in inhibition of tumor growth and metastasis. In all these models, striking changes in the composition of the tumor infiltrating leukocytes (TIL) at the primary or the metastatic tumor sites resulted from perturbation of PI3K. Moreover, these changes were partially responsible for the decrease in tumor growth and lung metastasis. Thus, co-treatment with BKM120 and the checkpoint inhibitor blockade, anti-PD1 antibody, resulted not only in enhanced reduction of tumor growth, but also significant tumor regression. Collectively, our data reveal that PI3K inhibition can not only inhibit tumor growth directly, but can also alter the host micro-environment to impair the growth of mammary tumor cells by increasing the population of anti-tumor leukocytes in the tumor. Moreover, our data suggest that the combination of PI3K inhibition across all isoforms and with checkpoint inhibitor PD-1 blockade may be highly beneficial for breast cancer patients.

Materials and Methods

Animals

Experiments were conducted in accordance with Vanderbilt University Animal Care and Use Committee guidelines (protocol number M/13/052). Generation of patient-derived xenograft (PDX) was approved by the Institutional Review Board (IRB number 130489). C57Bl/6, BALB/c and FVB wild type mice were purchased from Charles River. OT-I (C57BL/6-Tg (Tcr α Tcr β)1100Mjb/J) and OT-II (C57BL/6-Tg (Tcr α Tcr β)425Cbn/J) mutant mice were purchased from Jackson laboratory (Bar Harbor, Maine). Non-obese diabetic/severe combined immunodeficient (NOD/SCID)/interleukin-2 receptor γ chain null (NOD/SCID/IL2 γ^{null} , NSG) and NSG mice with beta-2 microglobulin deficiency (NSGB mice) were obtained from the Jackson Laboratory. PI3K γ knockout mice were from Jens Stein, University of Bern, Switzerland.

Materials

BKM120 was supplied by Novartis. The pharmacokinetics of BKM120 in mouse models has been previously described [20, 31]. Antibodies for CD8 depletion were from BioXCell (Lebanon, NH) as were anti-PD1 and the IgG control antibody. Antibodies for FACS analysis were from Biolegend, Inc. (San Diego, CA). All antibodies are Rat host, sourced from Biolegend, Inc., San Diego CA. Blocking Ab with TruStain fcXTM CD16/32(Clone#93), CD45(30-F11), CD19(6D5), CD3(17A2), CD4(RM4-5), CD8(53-6.7), CD25(PC61), CD11b(M1/70), CD11c(N418), Ly6c(HK1.4), Ly6g(1A8), CD49b(DX5), F4/80(BM8), MHCII(M5/114.15.2). Antibodies for immunohistochemistry were as follows: FoxP3 (FJK-16s) eBioscience, Inc., (San Diego, CA) 1:100; CD4 (4SM95) eBioscience, Inc., (San Diego, CA) 1:1000; CD8 (4SM15) eBioscience, Inc., (San Diego, CA) 1:1500; B220/CD45RO (RA3-6B2) BD- Pharmingen, (San Diego, CA) 1:200.

Implantation of breast tumor cells

MMTV-PyMT mammary tumor cells (C57/Bl/6 genetic background and FVBn background) were established from spontaneous tumors arising in mice [32]. 4T1 cells (BALB/c genetic background) were obtained from the ATCC. Cells were injected in the left fourth mammary fat pad of 6 – 8 week old non-parous female mice. Numbers of cells injected varied with cell type and experimental design. PDXs were generated by implanting 1–2mm diameter pieces of tumor tissue taken from TN breast cancer patients undergoing surgery or biopsy into NSGB mice obtained from Jackson Labs.

Evaluation of metastases

Hematoxylin and eosin (H&E) stained slides were reviewed by a pathologist using a standard microscope. The slides contained paraffin-embedded sections of lung tissue from the mice. Each slide was reviewed blinded and the number of metastases was counted. To ensure accuracy, the metastases on each slide were counted twice.

Treatment of mice bearing breast tumors with BKM120 or anti-PD-1

When the PyMT or 4T1 tumors became palpable (~2 weeks), mice were treated for 3 weeks with BKM120 (30 mg/Kg, QD) or vehicle by oral gavage. Tumor size (micro-caliper) and mouse weight were measured weekly. For anti-PD-1 experiments, PyMT cells were delivered to C57Bl/6 mice and when tumors grew to 10mm in length (~28 days) mice were treated with controls (DMSO and/or IgG2b), BKM120 (30mg/kg, daily), PD-1 antibody (100ug, on days 1 and 4 each week) for two weeks (day 42). Tumor size was measured twice weekly with microcalipers and tumor volume was calculated as $0.5 \times \text{length} \times \text{width} \times \text{width}$. After mice were euthanized, final tumor volume was determined by fluid displacement. Aliquots of tumor and lung were processed for FACS analysis of infiltrating leukocytes, for RNA or protein analysis, and for histology (see details in Supplemental Methods).

Statistical methods

Experiments designed to evaluate treatment effects on tumor growth were analyzed using mixed-effect models (Figure 1A, Figure 4A left panel, Supplement Figure 6C). The Wilcoxon rank sums test or the standard two sample t-test was used to compare outcome differences between two-group experiments. Standard analysis of variance with pairwise mean contrasts was used to analyze experiments with more than two groups. Quantitation of FACS populations was calculated by gating from single stained positive controls and fluorescence-minus-one (FMO) controls.

Results

BKM120 efficiently inhibited mammary tumor growth and metastasis

To evaluate the effects of a pan-class I PI3K inhibitor in a mammary tumor treatment model, BKM120 or vehicle were delivered to C57Bl/6 mice once palpable tumors were detected (about two weeks after orthotopic implantation of MMTV-PyMT mammary tumor cells (3×10^6)). BKM120 (30 mg/kg), or vehicle alone, was delivered to mice ($n = 5/\text{group}$) daily by oral gavage for 3 weeks. Tumors grew rapidly in vehicle control mice, while tumors in the mice treated with BKM120 stopped growing or grew very slowly (Figure 1A, $p < 0.0001$ mixed-effects model with a heterogeneous variance correction model for repeated measures with mean contrasts; day 26, $p = 0.0001$, day 33, 36, and 40, $p < 0.0001$). Western blot of representative mouse tumors and lungs revealed that the BKM120 did inhibit the level of p-AKT (S473) (Figure 1A, lower panel). Moreover, histological measurements of metastases in the lungs (Figure 1B lower panel) of tumor bearing mice showed a reduction in the tumor weight and a reduction in the number of metastases in the BKM120-treated mice after 3 weeks of treatment compared to vehicle control (Figure 1B ($p = 0.0088$, $p = 0.0071$, respectively, Wilcoxon Rank Sum test). We did not detect ($p < 0.05$) an association between tumor weight and number of metastases, adjusted for treatment ($p = 0.2948$, multivariable linear regression).

Similarly, we performed experiments in BALB/c mice with orthotopic implants of 4T1 breast cancer cells (5×10^4 cells) to examine the effects of BKM120 (30mg/kg daily, $n = 10$) versus vehicle control ($n = 10$). We observed no significant difference in tumor weight in the BKM120 treated versus vehicle control groups ($p = 0.06$, two sample t test on a log₂ scale),

but there was a significant decrease in lung metastasis ($p=0.0035$, two sample t-test on a log 2 scale) (Figures 1C and 1D) in the BKM120 treated group. Moreover, there was no significant linear association between tumor weight and number of metastasis, adjusted for treatment ($p\text{-value}=0.6228$ on a log2 scale). Also, there was no linear association between tumor weight and number of metastasis among BKM 120 treated group ($p=0.5739$ on a log2 scale) as well as among vehicle ($p=0.8661$ on a log2 scale) treated group.

We performed neutrophil chemotaxis assays (CXCL8 ligand, 0, 30, 300 ng/ml) in the presence or absence of BKM120 (0–1000nM) and as expected from our prior work, the migration of neutrophils isolated from mouse bone marrow was not significantly affected by PI3K inhibition (Figure 1 E) [33, 34]. To determine how BKM120 treatment affected tumor cell migration and invasion, we performed *in vitro* transwell invasion assays. Interestingly, the invasion of MMTV-PyMT mammary tumor cells toward 100ng/ml of CXCL12 was dramatically inhibited by BKM120 treatment (Figure 1 F, $p < 0.001$ for 300 nM of BKM120 vs. control and $p < 0.001$ for 1000nM of BKM120 vs. control). These data suggest that tumor cell extravasation from the blood vessels into the lung could be compromised by BKM120 treatment to reduce metastasis.

Leukocyte population infiltrated in primary tumor and lung

The leukocyte infiltrate is a key feature of the tumor stroma. The cytokine profile and composition of leukocyte infiltrate may turn the microenvironment into a “pro-tumor” or “anti-tumor” environment. Accordingly, we examined the changes in the intra-tumoral leukocyte population when PI3K was systemically inhibited by BKM120. While there were no significant changes in the total % of immune cells ($CD45^+$) in the tumor or lung after BKM120 treatment at the time tumors were harvested (Figure 2 A), when subpopulations of leukocytes in the tumor were examined there were significant decreases in the number of macrophages ($CD11b^+/CD11c^+/F4/80^+$) in the tumor but not the lung (Figure 2B). Moreover, BKM120 treatment resulted in an increase in the number of $CD4^+$ cells in the primary tumors ($p=0.05$), but not the lungs, with a trend toward an increase in $CD8^+$ T cells in tumor, but not lung (Figure 2 B). BKM120 treatment also produced an increase in the percentage of $IFN\gamma$ expressing $CD4^+$ T cells in the tumor (Figure 2 C, $p=0.05$), indicating a shift toward a Th1 phenotype. These group comparison were made using two sample t test.

Tumor cells can be killed directly by cytotoxic lymphocytes. To evaluate the effect of BKM120 treatment on T cell killing of tumor cells, T cell proliferation and cytotoxicity toward tumor cells was tested *in vitro* [35, 36]. Treatment of splenic cells with 300 nM BKM120, a concentration equivalent to the *in vivo* dosage used in these experiments, resulted in significant inhibition of $CD4^+$ ($p < 0.001$), but not $CD8^+$ T cell proliferation ($p > 0.05$) (Supplementary Figure 1A and 1B). In other experiments BALB/c mice were injected with 4T1 cells (1×10^6) then 3 days later BKM120 (30mg/kg) treatment was initiated. After 7 days of treatment $CD8^+$ T cells were isolated from the spleen and cytotoxicity assays were performed over an effector to target ratio of 0:1 to 50:1 (50 T cells for every 1 tumor cell). BKM120 did not significantly reduce the cytotoxicity of T cells toward target 4T1 tumor cells, $P > 0.05$, Wilcoxon rank sum test. (Supplementary Figure 1C). These data indicate that

pan-inhibition of PI3K may not interfere with proliferation or cytotoxic activity of CD8+ effector T cells.

Effects of BKM120 on the Leukocyte Population in the Pre-metastatic Niche

BKM120 inhibited 4T1 tumors in the formation of lung metastasis in BALB/c mice (Figure 1C) with a significant week by treatment effect ($p < 0.0001$, mixed effect model with heterogeneous variance correction on a nature log scale). To evaluate the possibility that BKM120 altered the pre-metastatic niche of the lung, non-tumor bearing BALB/c mice were treated with vehicle or BKM120 (30mg/kg, daily) for two weeks, then the leukocyte population in the lungs was analyzed by FACS. Four different populations of cells in the lung were identified based on expression of Ly6C and Ly6G on CD11b⁺ cells. There was a significant increase in the accumulation of CD11b⁺Ly6C⁺Ly6G^{low} leukocytes in the lungs of mice treated with BKM120 ($p = 0.005$, two sample t-test) and there was a decreased number of Ly6G^{low}Ly6C⁻ cells (Figure 3A). No differences in the number of T cells in the lung in response to BKM120 treatment were observed (two sample t-test).

Analysis of the gene expression profile of representative cytokines and chemokines (Figure 3B) from CD11b⁺Ly6C⁺Ly6G^{low} cells isolated from mouse lungs of non-tumor bearing mice revealed BKM120 increased IL-6 and CXCL11 and decreased CCL5 (RANTES) mRNA expression in the Ly6C⁺ cells isolated from the mouse lung. These data suggest the Ly6C⁺ cells may trend increasingly toward an anti-tumor (anti-metastatic) phenotype in the lung tissue after BKM120 treatment. Analysis of the phenotype of these cells showed changes in MHCII expression. Ly6C⁺ cells contain two subpopulations of cells, MHCII⁺ cells and MHCII⁻ cells, and BKM120 treatment decreased the number of MHCII⁺ cells as well as the expression of MHCII (Figure 3C). No significant changes were found in surface expression of CX3CR1, CXCR7, CD49a ($\alpha 1$), $\beta 6$, CD49e ($\alpha 5$), CD51, CD197, CD61, CD49f ($\alpha 6$), CD126, F4/80, $\beta 6$, CD49b, CD124, CD80, CD49f, CD184, CD49d, CD86, Cd244, CD182, CD81, CD11c, CD115 and CD104 (data not shown).

To determine whether BKM120 was affecting the differentiation of mouse or human bone marrow cells into Ly6C⁺ cells, *in vitro* experiments were performed. Bone marrow cells were differentiated into myeloid cells in the presence of GM-CSF (20ng/ml) with either BKM120 or vehicle for 5 days. Results show that BKM120 treatment of mouse and human bone marrow cells resulted in a ~25% increase in Ly6C⁺ (mouse) and CD14⁺CD1a^{low} (human) cells, respectively (Figure 3D). Altogether, these data indicate that BKM120 can influence the differentiation of bone marrow progenitors and can increase the Ly6C⁺ population of cells in the pre-metastatic niche of the lung, shifting these cells toward a more pro-inflammatory phenotype to impair metastasis formation (Figure 3).

The inhibition of tumor growth and metastasis is diminished if BKM120 treatment is paused then re-initiated

One possible explanation for the reduction in tumor metastasis in mice treated with BKM120 is that the primary tumors were smaller in size and number in the treatment group than the tumors in the control group and as a result had not reached sufficient size for metastasis. To test this possibility, we allowed PyMT tumors in BKM120 treated C57Bl/6

mice to grow to the same size as the control group prior to sacrifice and analyzed metastatic lung lesions. In another group of mice, BKM120 treatment was paused for two weeks and then either reinitiated or not reinitiated in the two treatment subgroups. For treatment-paused mice, tumors grew rapidly after suspension of BKM120 treatment, and once treatment resumed, rapid tumor growth continued. Tumors from mice that received continuous BKM120 treatment for 7 weeks exhibited a growth curve that was slower than the vehicle control group, when we compared the linear component of the two growth curves ($P=0.005$) (Supplementary Figure 2). There was no difference in number of metastatic lesions in the lung for all the groups of mice that received different periods of BKM120 treatment (data not shown). However, one caveat for this experimental design is the BKM120 treated tumors have been growing for a longer time, thus allowing increased time for metastasis, so we cannot conclude from this experiment that metastasis frequency is directly related to tumor size. Moreover, as noted in the 4T1/BALB/c model in Figure 1 C and D, even within the vehicle control group there was no statistically significant relationship between tumor volume and number of metastasis.

Effects of combined BKM120 and anti-PD1 on the growth of PyMT tumors

BKM120 treatment of mice bearing breast tumors results in alteration of immune cells in the tumor microenvironment. We hypothesized that combining BKM120 treatment with the check-point inhibitor, anti-PD1, would result in enhanced reduction in tumor growth. First, however we evaluated whether inhibition of PI3K would affect PD-L1 expression by tumor cells or PD-1 expression by T cells. We treated MMTV-PyMT tumor cells with IFN- γ and either BKM120 or vehicle for 24 hours then examined the surface expression of PDL1 in MMTV-PyMT tumor cells. We did not see any changes in PD-L1 expression on MMTV-PyMT cells after BKM120 treatment (Supplementary Figure 3A). We also observed no changes for the PD-1 expression in T lymphocytes after treatment with BKM120 or vehicle control and stimulated with the plant lectin Concanavalin A, a mitogen for mouse T-cell subsets, for 3 days *in vitro* (Supplementary Figure 3B).

Based upon these results, we determined whether combining BKM120 and anti-PD1 would result in greater inhibition of tumor growth than with either agent alone. C57Bl/6 female non-parous mice (10 weeks of age) were implanted orthotopically into the fourth mammary gland with 50,000 syngeneic PyMT cells. When tumors reached a size of ~1cm in any direction (~4 weeks), mice were either treated with Vehicle, IgG, vehicle + IgG, or α PD-1 blocking antibody (100 μ g twice a week on days 1 and 4), BKM-120 (30mg/kg daily) or a combination of both α PD-1 and BKM-120 for two weeks. Tumor measurements over the treatment period showed significant reduction in growth with BKM120 alone (Holm adj $p<0.0001$, mixed-effects model comparing least square (model predicted) means, Figure 4A) and the addition of anti-PD1 resulted in a significantly smaller mean tumor volume than with BKM120 treatment alone (Holm adj. $p<0.001=0.0002$, mixed-effects model as above, Figure 4A) ($n=10$). Comparisons between average tumor volume (\pm SE.) at the 14th day revealed that differences in average tumor volume between BKM120+anti-PD1 and BKM120 were statistically significantly (Holm adj. $p<0.011$), while differences for each in comparison to vehicle control or vehicle plus IgG2b were also statistically significant (Holm adj. $p<0.001$ and adj. $p<0.001$, one way-ANOVA with model predicted mean contrasts,

Figure 4A right panel). The histology of the primary tumors typified PyMT tumors as advanced adenocarcinomas with enhanced presence of B-cells, CD8 T-cells and FoxP3+ cells in BKM120 and the combined BKM120 and PD-1 antibody treated tumors (Figure 4B). Quantification of FoxP3 IHC for both peritumoral area and intratumoral area revealed distinct accumulation of FoxP3+ cells in BKM120 (20x Field of View) compared with combined treatment (Figure 4C). FACS analysis of immune cells infiltrating the tumors after therapy revealed an increase in the leukocyte content in α PD-1, BKM120 or combined treatments. There were significant increases in B-cell, T-cell and CD4+/CD25+ cells in BKM120 alone treated tumors, and addition of α PD-1 to the BKM120 treatment further increased the B cell infiltrate and reduced the BKM120 increase in CD4+/CD25+ cells (Figure 4D and Supplemental Figure 3C and 3D). There was no difference in the viability of immune cells between the four treatment groups. BKM120 alone and BKM120+anti-PD1 tended to increase the NK cell population (CD49b+ CD45+) as compared to control or anti-PD1 alone; the combination treatment also tended to reduce the neutrophil population (Ly6g/CD11b+) and increase the % Ly6C+/Ly6G+ CD11b cells. Each of the three treatments tended to increase F4/80/MHCII+ CD45 cells compared to vehicle control (Supplementary Figure 3E). Also, immunohistochemical analysis of tumor tissues after treatment with anti-PD1, BKM120, or the combination revealed that the BKM120, but not anti-PD1 or the combined treatment increased the FoxP3 content around the edges of the tumor, while the combined treatment resulted in increased intratumoral FoxP3 cells. Neither of the treatments affected the splenic distribution of FoxP3 cells. Moreover, BKM120 increased the tumoral CD4+ T cell content, but the combination treatment diminished this (Supplemental Figure 3F).

BKM120 treatment results in increased desmoplasia and a fibrotic tumor microenvironment

One of the more notable histological observations in tumors treated with BKM120 was the accumulation of reactive stroma (Supplemental Figure 4A). BKM120 treated tumors also had a noticeable increase in collagen accumulation and maturation within the tumor as demonstrated by trichrome and picroSirius red staining (Supplemental Figure 4A). An immunofluorescent staining of tumors revealed cancer-associated-fibroblast (CAF) markers α SMA and vimentin were more densely distributed within the BKM120 treated tumors (Supplemental Figure 4B). To investigate the effect of BKM120 on CAFs, we established three primary fibroblast cell lines from PyMT mouse tumors and treated these with BKM120 (1 μ M for 24h), or vehicle. Treatment of three cell lines established from 3 different mice resulted in a significant increase in *II4* and *Ccl5* mRNA (Supplemental Figure 4C, $p < 0.05$). Primary fibroblasts cultures established from mammary glands of PI3K γ null mice also had elevated *II4* and *ccl5* expression (Supplemental Figure 4D, $p < 0.05$ and $p < 0.01$, respectively). When we established primary human fibroblast cultures from mammary reduction we found that treatment with the PI3K γ -specific inhibitor, AS605240, also significantly elevated *II4* and *ccl5* gene expression (Supplemental Figure 4E, $p < 0.5$). Altogether these results indicate that reduced tumor growth resulting from PI3K inhibition is accompanied by a desmoplastic event that triggers an inflammatory tumor microenvironment.

Growth of orthotopic implants of human breast tumor tissue into humanized NSG mice is inhibited by BKM120

The findings with MMTV-PYMT mouse tumors prompted us to test how BKM120 affects tumor growth and anti-tumor immunity in a human breast cancer model. We used a “humanized mouse” model in which tumors from triple negative breast cancer (TNBC) patients were orthotopically implanted into the mammary fat pad of NSGB mice that were engrafted with the same patient’s CD34+ HSCs followed by infusion with the patient’s CD4 (hCD4+) and CD8+ (hCD8+) T cells (Supplemental Figure 5 and Supplemental Methods). Tumor bearing mice treated with BKM120 exhibited a reduction of tumor-infiltrating hCD4+ T cells ($57 \pm 4.4\%$ vs. $30 \pm 4.3\%$), but of the hCD4+ cells detected, there was an increase in the percent that were activated (CD4⁺CD69⁺ cells, $3.7 \pm 1.2\%$ in vehicle vs. $38 \pm 3.9\%$ in BKM120 treated) (Supplemental Figure 6A). Similarly, the percentage of the human CD45+ cells that were human B-cells (hB) tended to increase in BKM120-treated engrafted mice (CD20⁺ cells, $3 \pm 0.8\%$ vs. $11 \pm 3.4\%$), but the increase did not achieve statistical significance (Supplemental Figure 6A). BKM120 did not affect the CD8+CD107+ T cells, which were quite scarce in the tumors. BKM120 inhibition of the PI3K signaling pathway promoted activation of hCD4+ T cells based upon CD69 staining ($p < 0.01$) and increased the infiltration of hB cells (Supplemental Figure 6B), leading to a switch in the CD4⁺T cell lineage phenotype to anti-tumor immunity. There was significant inhibition of tumor growth by the third and fourth weeks of treatment with BKM120 ($p < 0.0001$, mixed-effects model with heterogenous variance correction) (Supplemental Figure 6C). Similar results were obtained with a second TNBC engrafted and treated (data not shown). Therefore, the results with this humanized mouse model with an orthotopic PDX are similar to that with the PyMT and 4T1 mouse tumor models, where PI3K inhibition arrested tumor cell growth and provided a more anti-tumor milieu, though in the humanized mouse model we saw a reduction in total CD4⁺T cells and a shift to an anti-tumor phenotype (CD4⁺/CD69⁺) for the CD4⁺ T cells infiltrating the tumor.

The tumor growth and metastasis are inhibited in PI3K γ ^{-/-} mice

Since PI3K γ is the major subtype involved in leukocyte chemotaxis, to investigate how loss of PI3K γ only in the non-tumor cells of the host impacted tumor growth and metastasis, we evaluated the growth of the PI3K γ -wild type (WT) MMTV-PyMT tumor cells in PI3K γ ^{-/-} mice. We hypothesized that the loss of PI3K γ in the TME might alter recruitment of subsets of leukocytes to the tumor and lung, and therefore change the TME to affect growth of the primary tumor and metastasis to secondary organ sites. Five weeks after implantation of MMTV-PyMT into the mammary fat pad, the tumors in PI3K γ ^{-/-} mice grew much slower than those in the C57BL/6 PI3K γ WT wild-type mice ($800 \pm 75 \text{ mm}^3$ in WT vs. $400 \pm 50 \text{ mm}^3$ in PI3K γ ^{-/-} $p < 0.01$, two sample t-test) (Figure 5A). The number of lung metastasis was also significantly reduced in PI3K γ ^{-/-} mice, much like what was observed with BKM120 treatment ($p < 0.01$, two sample t-test; Figure 5B). These results suggest that the loss of PI3K γ only in the host non-tumor cells is sufficient to inhibit tumor growth and metastasis.

PI3K $\gamma^{-/-}$ mice exhibited increased leukocyte recruitment into the tumor compared to PI3K γ WT mice

We observed similarly that with systemic PI3K inhibition by BKM120 treatment, the infiltration of PMN/iMC into the primary tumors was significantly increased in PI3K $\gamma^{-/-}$ mice (Figure 5C). Furthermore, significantly more CD4 $^{+}$ ($p < 0.05$), CD8 $^{+}$ T cells ($p < 0.05$) and CD19 $^{+}$ B cells ($p < 0.05$) were found in primary tumors in PI3K $\gamma^{-/-}$ mice (Figure 5D). In lungs of tumor bearing PI3K $\gamma^{-/-}$ mice, the infiltration of lymphoid cells (CD8 $^{+}$ T cells or B cells) was significantly increased (CD8 $^{+}$ T cells $p = 0.002$; B cells $p = 0.019$) and there was also an increased number of monocytes (CD11b $^{+}$ F4/80-Gr1 $^{-}$, $p = 0.019$). Of note, since there are more lymphoid cells in the bone marrow and spleen of PI3K $\gamma^{-/-}$ compared to WT mice (Supplementary Figure 7A, 7B, Wilcoxon rank sum test, * $p < 0.05$), this could provide more lymphoid cells to infiltrate primary tumors and lungs. These data also suggest that PI3K γ activity may play some role in suppressing the generation of lymphoid cells and when this is lost, these cells are increased in the spleen and bone marrow.

Also we found significant differences in IFN γ and TNF α secretion by CD8 and CD4 cells in tumor and lungs (Figure 5E, F). Significantly more CD8 and CD4 cells were producing TNF α in tumor tissue and lungs from PI3K $\gamma^{-/-}$ mice: (CD4 $^{+}$ T cells, $p = 0.018$ and CD8 $^{+}$ T cells, $p = 0.001$). A marginal effect was found in the production of IFN γ by CD8 cells in lungs of PI3K $\gamma^{-/-}$ mice (Figure 5E) and TNF α by CD8 cells in tumor tissue (Figure 5F). To test whether PI3K $\gamma^{-/-}$ loss in neutrophils and lymphocytes can impair the chemotaxis of these cells toward a gradient of chemokine, the chemotactic index of neutrophils isolated from bone marrow and of lymphocytes isolated from spleens of PI3K $\gamma^{-/-}$ mice or WT mice were tested in a modified Boyden chamber assay [37]. The chemotactic index in response to CXCL8 was not significantly different between the PI3K $\gamma^{-/-}$ and PI3K γ WT mice (Supplementary Figure 7C), confirming our prior observations that leukocyte chemotaxis can occur in a PI3K-independent manner [33]. Moreover, lymphocytes isolated from PI3K $\gamma^{-/-}$ mice exhibited a migration toward CXCL12 that was not impaired and basal migration appeared to be enhanced compared to control (Supplemental Figure 7D).

Depletion of CD8 $^{+}$ T cells resulted in partial restoration of tumor growth in PI3K $\gamma^{-/-}$ mice

To determine whether the elevation in CD8 $^{+}$ T cells in PI3K $\gamma^{-/-}$ mice contributed to the inhibition of tumor growth and metastasis to the lung, we depleted CD8 $^{+}$ T cells from these mice by intraperitoneal injection of anti-CD8 antibody (100 μ g for 3 consecutive days, then every other day for 3 weeks) and confirmed the depletion of CD8 $^{+}$ T cells by flow cytometry analysis of lung and spleen (Figure 6A). In the lungs of WT mice, CD8 $^{+}$ cells as a percentage of total CD90 $^{+}$ cells were reduced from 29.5 \pm 4.2% to 9.2 \pm 2.6%, while in spleen, the reduction was from 12.9 \pm 1.6% to 3.6 \pm 0.9% after application of antibody for 3 weeks. In the lungs of PI3K $\gamma^{-/-}$ mice, CD8 $^{+}$ cells decreased from 43.2 \pm 1.4% to 4.6 \pm 0.8%, while in spleen, the decrease of CD8 $^{+}$ T cells was from 16.5 \pm 0.8% to 2.0 \pm 0.3 (Figure 6A for representative FACS analysis and graph showing data from each mouse). We also evaluated the effect of CD8 IgG on the CD4 $^{+}$ T cell population. Differences in the CD4 $^{+}$ T cell population in the lung (31.9 \pm 1.7 (isotype control) versus 52.9 \pm 1.1 (CD8 IgG) but not the spleen were observed in the PI3K $\gamma^{-/-}$ mice after mice were treated with CD8 IgG, but there were no differences in the CD4 $^{+}$ cells in WT mice in the lung or the spleen (Figure

6A). Interestingly, there was no statistical difference between growth rates of tumors in WT mice with or without CD8⁺ T cell depletion. However, in PI3K γ ^{-/-} mice, depletion of CD8⁺ T cells resulted in significantly larger tumor size than those without CD8⁺ T cell depletion ($p < 0.05$ two-way ANOVA with Bonferroni post-tests at day 35). This finding indicates that the increased presence of activated CTL in a tumor micro-environment lacking PI3K γ inhibits tumor growth. Although tumor growth in PI3K γ ^{-/-} mice with depletion of CD8⁺ T cells resulted in enhanced tumor growth compared to isotype antibody control, the fact that growth equal to that of WT mice did not ensue suggests that other factors and other cells in addition to CD8⁺ T cells contributed to the inhibition of tumor growth ($p < 0.001$ two sample t-test $p < 0.05$ at day 24, $p < 0.001$ at day 31 and 35) (Figure 6B). As an additional issue, there was no statistically significant difference in lung metastasis frequencies of the mice treated with IgG control or anti-CD8 antibody which is likely related to the sparsity of CD8T cells in control tumors ($p > 0.05$, two sample t-test) (Figure 6C). Notwithstanding these caveats, the crucial finding from these experiments is that loss of PI3K γ in the tumor microenvironment alone results in an inhibition of tumor growth.

Discussion

PI3K activity is very important for both tumor progression and the immune cell activity, and systemic inhibitors of various PI3Ks have recently been developed for clinical use [17, 19, 38]. Inhibition of PI3K α alone may not be effective in luminal breast cancer due to a rebound reactivation of class IA PI3K via PI3K β [39]. In this study, we showed in three different orthotopic mammary cancer mouse allograft and xenograft models that treatment with a pan PI3K inhibitor, BKM120, markedly inhibited tumor growth and number of metastases while at the same time increased the migration of myeloid cells into the tumor. In the 4T1 and PyMT models there was no statistical association between tumor growth and number of metastases, but in the PyMT model, if BKM120 treated tumors were allowed to grow to the same size as vehicle control prior to sacrifice, no difference in numbers of metastasis was observed. Thus it is possible that in the PyMT tumors BKM120 appeared to decrease the number of metastases by decreasing primary tumor growth/burden. However, since these tumors were growing for a longer period of time, the loss of an effect on metastasis might be the result of a longer growing period. BKM120 did not significantly alter the number of CD8⁺T cells migrating into the tumor, but did increase the percentage of intra-tumoral CD4⁺T cells and of those a greater percentage produced IFN- γ . Prior work from Marshall *et al.* support our findings that PI3K inhibitors can alleviate immune suppression by promoting IFN γ -secreting, anti-tumor T cells [40]. We show that BKM120 also enhanced the differentiation of myeloid cells towards a monocytic lineage (Ly6C⁺Ly6G⁻F4/80⁻ in mice, CD14⁺CD1a^{dim} in human) with an increased accumulation of these pro-inflammatory cells in the lungs of non-tumor bearing mice. At the same time BKM120 impaired the invasive migration of tumor cells.

Our results also indicate that PI3K γ activity in the stromal cells of the tumor microenvironment plays a key role in tumor cell proliferation and migration. Loss of PI3K γ activity in the host was associated with dramatically increased infiltration of CD4⁺ and CD8⁺ T lymphocytes and PMN/iMC into the PI3K γ ^{WT} tumor; in lung there was also a major increase in infiltrating CD8⁺T lymphocytes, CD4⁺ T lymphocytes, and Tregs, but a

decrease in PMN/IMCs and DCs that correlated with the decrease in lung metastasis. The tumor and lung infiltrating CD8⁺ T cells expressed IFN- γ and TNF α , indicating a strong anti-tumor environment was present. While we cannot rule out the possibility that some of the changes in the leukocyte populations are linked to decreased tumor size, since in other tumor models smaller tumors exhibit an influx of CD4⁺ and CD8⁺ T cells which is followed by a decline in these T cells and an increase in neutrophils and macrophages as the tumor grows [41]. Our results with PI3K $\gamma^{-/-}$ mice are somewhat similar to results from mice expressing inactive PI3K δ (p110 δ^{D910A}) where growth and metastasis of B16 melanoma (C57Bl/6), Lewis lung carcinoma (C57Bl/6) and 4T1 breast cancer (BALB/c) were inhibited [10]. Similar results were obtained with a P110 δ -specific inhibitor. Additionally, as we have shown with PI3K $\gamma^{-/-}$ mice, in their model depletion of CD8⁺ T cells removed the tumor response to the P110 δ -specific inhibitor [10].

We report here that treatment with BKM120 efficiently inhibited MMTV-PyMT, 4T1 and TNBC PDX cancer growth and/or metastasis. Clinical trial results from Ma *et al* reported that BKM120 was somewhat effective in treating ER⁺ breast cancer patients who did not exhibit loss of PTEN, loss of progesterone receptor expression, or mutation in *TP53* [14]. Moreover, response did not correlate with *PI3KCA* mutation and mutation in *AKT1* or *ESR1* did not ablate response [14]. As is the case for other single agent treatments for breast cancer, sustained PI3K inhibition results in development of tumor cell resistance to PI3K inhibitor therapy [15, 42].

To potentially avoid this resistance, we considered combining BKM120 with other agents, such as blockade of immune checkpoint inhibitors. In our studies with PI3K γ null mice, depletion of CD8⁺T cells partially restored the anti-tumor response against the PyMT tumors. Kaneda et al showed that blockade of PI3K γ reprograms tumor associated macrophages toward a Th1 program to enhance CD8⁺T-cell-mediated suppression of tumor growth and metastasis [43] [41]. In fact, they showed that PI3K γ activation results in a negative feedback to inhibit NF- κ B mediated production of key chemokines that recruit T cells [41].

Our findings also support the findings of Peng *et al* that PI3K activity participates in development of resistance to T cell immunotherapy (50). Considering our data in the context of work from Marshall [40] and Peng [44], it was be important to consider combining a pan-PI3K inhibitor with immune checkpoint inhibitors for treatment of breast cancers. Here we show that anti-PD1 was not effective as a monotherapy in the PyMT breast cancer model, but combining BKM120 with anti-PD1 further reduced tumor growth over that observed with BKM120 treatment alone and resulted in blockage of tumor growth in 100% of the mice. In contrast to our data, Kanada *et. al.* showed that PI3K γ inhibitor plus anti-PD1 was ineffective for treatment of pancreatic cancers in mice, but that combining PI3K γ inhibitors with standard of care chemotherapy and anti-PD1 slowed the growth of pancreatic cancer (41). The difference between the two studies could be due to differences in use of a pan-PI3K inhibitor that will target breast tumor cells versus a PI3K γ specific inhibitor that does not directly target pancreatic tumor cells. Our data show for the first time that combining pan-PI3K inhibition with antibody to the checkpoint inhibitor PD1 markedly impairs breast tumor growth and induces tumor regression. These data should lead the way to new clinical

6. Perez-Tenorio G, Alkhorri L, Olsson B, Waltersson MA, Nordenskjold B, Rutqvist LE, et al. PIK3CA mutations and PTEN loss correlate with similar prognostic factors and are not mutually exclusive in breast cancer. *Clin Cancer Res.* 2007; 13(12):3577–3584. [PubMed: 17575221]
7. Kalinsky K, Jacks LM, Heguy A, Patil S, Drobnjak M, Bhanot UK, et al. PIK3CA mutation associates with improved outcome in breast cancer. *Clin Cancer Res.* 2009; 15(16):5049–5059. [PubMed: 19671852]
8. Cizkova M, Susini A, Vacher S, Cizeron-Clairac G, Andrieu C, Driouch K, et al. PIK3CA mutation impact on survival in breast cancer patients and in ERalpha, PR and ERBB2-based subgroups. *Breast Cancer Res.* 2012; 14(1):R28. [PubMed: 22330809]
9. Saal LH, Holm K, Maurer M, Memeo L, Su T, Wang X, et al. PIK3CA mutations correlate with hormone receptors, node metastasis, and ERBB2, and are mutually exclusive with PTEN loss in human breast carcinoma. *Cancer Res.* 2005; 65(7):2554–2559. [PubMed: 15805248]
10. Ali K, Soond DR, Pineiro R, Hagemann T, Pearce W, Lim EL, et al. Inactivation of PI(3)K p110delta breaks regulatory T-cell-mediated immune tolerance to cancer. *Nature.* 2014; 510(7505):407–411. [PubMed: 24919154]
11. Chakrabarty A, Bhola NE, Sutton C, Ghosh R, Kuba MG, Dave B, et al. Trastuzumab-resistant cells rely on a HER2-PI3K-FoxO-survivin axis and are sensitive to PI3K inhibitors. *Cancer Res.* 2013; 73(3):1190–1200. [PubMed: 23204226]
12. Chakrabarty A, Sanchez V, Kuba MG, Rinehart C, Arteaga CL. Feedback upregulation of HER3 (ErbB3) expression and activity attenuates antitumor effect of PI3K inhibitors. *Proc Natl Acad Sci U S A.* 2011; 109(8):2718–2723. [PubMed: 21368164]
13. Klarenbeek S, van Miltenburg MH, Jonkers J. Genetically engineered mouse models of PI3K signaling in breast cancer. *Mol Oncol.* 2013; 7(2):146–164. [PubMed: 23478237]
14. Ma CX, Luo J, Naughton M, Ademuyiwa FO, Suresh R, Griffith M, et al. A phase I trial of BKM120 (Buparlisib) in combination with fulvestrant in postmenopausal women with estrogen receptor positive metastatic breast cancer. *Clin Cancer Res.* 2015; 22:1583–1591. [PubMed: 26563128]
15. Vora SR, Juric D, Kim N, Mino-Kenudson M, Huynh T, Costa C, Lockerman EL, Pollack SF, Liu M, Li X, et al. CDK 4/6 inhibitors sensitize PIK3CA mutant breast cancer to PI3K inhibitors. *Cancer Cell.* 2014; 26(1):136–149. [PubMed: 25002028]
16. Leroy C, Amante RJ, Bentires-Alj M. Anticipating mechanisms of resistance to PI3K inhibition in breast cancer: a challenge in the era of precision medicine. *Biochem Soc Trans.* 2014; 42(4):733–741. [PubMed: 25109950]
17. Folkes AJ, Ahmadi K, Alderton WK, Alix S, Baker SJ, Box G, et al. The identification of 2-(1H-indazol-4-yl)-6-(4-methanesulfonyl-piperazin-1-ylmethyl)-4-morpholin-4-yl-1H-imidazo[3,2-d]pyrimidine (GDC-0941) as a potent, selective, orally bioavailable inhibitor of class I PI3 kinase for the treatment of cancer. *J Med Chem.* 2008; 51(18):5522–5532. [PubMed: 18754654]
18. O'Brien C, Wallin JJ, Sampath D, GuhaThakurta D, Savage H, Punnoose EA, et al. Predictive biomarkers of sensitivity to the phosphatidylinositol 3' kinase inhibitor GDC-0941 in breast cancer preclinical models. *Clin Cancer Res.* 2010; 16(14):3670–3683. [PubMed: 20453058]
19. Maira SM, Pecchi S, Huang A, Burger M, Knapp M, Sterker D, et al. Identification and characterization of NVP-BKM120, an orally available pan-class I PI3-kinase inhibitor. *Mol Cancer Ther.* 2012; 11(2):317–328. [PubMed: 22188813]
20. Geuna E, Milani A, Martinello R, Aversa C, Valabrega G, Scaltriti M, Montemurro F. Buparlisib, an oral pan-PI3K inhibitor for the treatment of breast cancer. *Expert Opin Investig Drugs.* 2015; 24(3):421–431.
21. Yuan TL, Cantley LC. PI3K pathway alterations in cancer: variations on a theme. *Oncogene.* 2008; 27(41):5497–5510. [PubMed: 18794884]
22. Adams S, Gray RJ, Demaria S, Goldstein L, Perez EA, Shulman LN, et al. Prognostic value of tumor-infiltrating lymphocytes in triple-negative breast cancers from two phase III randomized adjuvant breast cancer trials: ECOG 2197 and ECOG 1199. *J Clin Oncol.* 2014; 32(27):2959–2966. [PubMed: 25071121]
23. Okkenhaug K, Vanhaesebroeck B. PI3K–signalling in B- and T-cells: insights from gene-targeted mice. *Biochem Soc Trans.* 2003; 31(Pt 1):270–274. [PubMed: 12546700]

24. Reif K, Okkenhaug K, Sasaki T, Penninger JM, Vanhaesebroeck B, Cyster JG. Cutting edge: differential roles for phosphoinositide 3-kinases, p110gamma and p110delta, in lymphocyte chemotaxis and homing. *J Immunol.* 2004; 173(4):2236–2240. [PubMed: 15294934]
25. Pardoll DM. The blockade of immune checkpoints in cancer immunotherapy. *Nat Rev Cancer.* 2012; 12(4):252–264. [PubMed: 22437870]
26. Wolchok JD, Hodi FS, Weber JS, Allison JP, Urba WJ, Robert C, et al. Development of ipilimumab: a novel immunotherapeutic approach for the treatment of advanced melanoma. *Ann N Y Acad Sci.* 2013; 1291:1–13. [PubMed: 23772560]
27. Topalian SL, Hodi FS, Brahmer JR, Gettinger SN, Smith DC, McDermott DF, et al. Safety, activity, and immune correlates of anti-PD-1 antibody in cancer. *N Engl J Med.* 2012; 366(26):2443–2454. [PubMed: 22658127]
28. Darcy PK, Neeson P, Yong CS, Kershaw MH. Manipulating immune cells for adoptive immunotherapy of cancer. *Curr Opin Immunol.* 2014; 27:46–52. [PubMed: 24534448]
29. Granot Z, Henke E, Comen EA, King TA, Norton L, Benezra R. Tumor entrained neutrophils inhibit seeding in the premetastatic lung. *Cancer Cell.* 2011; 20(3):300–314. [PubMed: 21907922]
30. Melero I, Berman DM, Aznar MA, Korman AJ, Perez Gracia JL, Haanen J. Evolving synergistic combinations of targeted immunotherapies to combat cancer. *Nat Rev Cancer.* 2015; 15(8):457–472. [PubMed: 26205340]
31. Bendell JC, Rodon J, Burris HA, de Jonge M, Verweij J, Birlle D, et al. Phase I, dose-escalation study of BKM120, an oral pan-Class I PI3K inhibitor, in patients with advanced solid tumors. *J Clin Oncol : off.* 2012; 30(3):282–290.
32. Pickup MW, Hover LD, Polikowsky ER, Chytil A, Gorska AE, Novitskiy SV, Moses HL, Owens P. BMP2 loss in fibroblasts promotes mammary carcinoma metastasis via increased inflammation. *Mol Oncol.* 2015; 9(1):179–191. [PubMed: 25205038]
33. Sai J, Raman D, Liu Y, Wikswo J, Richmond A. Parallel phosphatidylinositol 3-kinase (PI3K)-dependent and Src-dependent pathways lead to CXCL8-mediated Rac2 activation and chemotaxis. *J Biol Chem.* 2008; 283(39):26538–26547. [PubMed: 18662984]
34. Liu B, Ma Y, Zhang Y, Zhang C, Yi J, Zhuang R, Yu H, Yang A, Jin B. CD8 low CD100- T Cells Identify a Novel CD8 T Cell Subset Associated with Viral Control during Human Hantaan Virus Infection. *J Virol.* 2015; 89(23):11834–11844. [PubMed: 26378166]
35. Shrikant P, Khoruts A, Mescher MF. CTLA-4 blockade reverses CD8+ T cell tolerance to tumor by a CD4+ T cell- and IL-2-dependent mechanism. *Immunity.* 1999; 11(4):483–493. [PubMed: 10549630]
36. Zhang X, Huang H, Yuan J, Sun D, Hou WS, Gordon J, Xiang J. CD4-8- dendritic cells prime CD4+ T regulatory 1 cells to suppress antitumor immunity. *J Immunol.* 2005; 175(5):2931–2937. [PubMed: 16116179]
37. Boyden S. The chemotactic effect of mixtures of antibody and antigen on polymorphonuclear leucocytes. *J Exp Med.* 1962; 115:453–466. [PubMed: 13872176]
38. Hoeflich KP, Merchant M, Orr C, Chan J, Den Otter D, Berry L, et al. Intermittent administration of MEK inhibitor GDC-0973 plus PI3K inhibitor GDC-0941 triggers robust apoptosis and tumor growth inhibition. *Cancer Res.* 2012; 72(1):210–219. [PubMed: 22084396]
39. Costa C, Ebi H, Martini M, Beausoleil SA, Faber AC, Jakubik CT, et al. Measurement of PIP3 levels reveals an unexpected role for p110beta in early adaptive responses to p110alpha-specific inhibitors in luminal breast cancer. *Cancer Cell.* 2015; 27(1):97–108. [PubMed: 25544637]
40. Marshall NA, Galvin KC, Corcoran AM, Boon L, Higgs R, Mills KH. Immunotherapy with PI3K inhibitor and Toll-like receptor agonist induces IFN-gamma+IL-17+ polyfunctional T cells that mediate rejection of murine tumors. *Cancer Res.* 2012; 72(3):581–591. [PubMed: 22158905]
41. Kaneda MM, Cappello P, Nguyen AV, Ralainirina N, Hardamon CR, Foubert P, et al. Macrophage PI3Kgamma Drives Pancreatic Ductal Adenocarcinoma Progression. *Cancer Discovery.* 2016; 6(8):870–885. [PubMed: 27179037]
42. Rozenfurt E, Soares HP, Sinnet-Smith J. Suppression of Feedback Loops Mediated by PI3K/mTOR Induces Multiple Overactivation of Compensatory Pathways: An Unintended Consequence Leading to Drug Resistance. *Mol Cancer Ther.* 2014; 13(11):2477–2488. [PubMed: 25323681]

43. Gunderson AJ, Kaneda MM, Tsujikawa T, Nguyen AV, Affara NI, Ruffell B, et al. Bruton Tyrosine Kinase-Dependent Immune Cell Cross-talk Drives Pancreas Cancer. *Cancer discovery*. 2016; 6(3): 270–285. [PubMed: 26715645]
44. Peng J, Tsang JY, Ho DH, Zhang R, Xiao H, Li D, et al. Modulatory effects of adiponectin on the polarization of tumor-associated macrophages. *Intl J Cancer*. 2015; 137(4):848–858.
45. Bedard PL, Taberero J, Janku F, Wainberg ZA, Paz-Ares L, Vansteenkiste J, et al. A phase Ib dose-escalation study of the oral pan-PI3K inhibitor buparlisib (BKM120) in combination with the oral MEK1/2 inhibitor trametinib (GSK1120212) in patients with selected advanced solid tumors. *Clin Cancer Res*. 2015; 21(4):730–738. [PubMed: 25500057]
46. Nanda R, Chow LQ, Dees EC, Berger R, Gupta S, Geva R, et al. Pembrolizumab in Patients With Advanced Triple-Negative Breast Cancer: Phase Ib KEYNOTE-012 Study. *J Clin Oncol*. 2016; 34(21):2460–2467. [PubMed: 27138582]
47. Emens LAF, Cassier P, Delord J, Eder JP, Fasso M, Xiao Y, et al. Inhibition of PD-L1 by MPDL3280A leads to clinical activity in patients with metastatic triple-negative breast cancer (TNBC). *Cancer Res*. 2015; 75(15 Suppl):2859.
48. Migali C, Milano M, Trapani D, Criscitiello C, Esposito A, Locatelli M, et al. Strategies to modulate the immune system in breast cancer: checkpoint inhibitors and beyond. *Ther Adv Med Oncol*. 2016; 8(5):360–374. [PubMed: 27583028]
49. Beckers RK, Selinger CI, Vilain R, Madore J, Wilmott JS, Harvey K, et al. Programmed death ligand 1 expression in triple-negative breast cancer is associated with tumour-infiltrating lymphocytes and improved outcome. *Histopathol*. 2016; 69(1):25–34.
50. Ali HR, Glont SE, Blows FM, Provenzano E, Dawson SJ, Liu B, et al. PD-L1 protein expression in breast cancer is rare, enriched in basal-like tumours and associated with infiltrating lymphocytes. *Ann Oncol/ ESMO*. 2015; 26(7):1488–1493.
51. Sabatier R, Finetti P, Mamessier E, Adelaide J, Chaffanet M, Ali HR, et al. Prognostic and predictive value of PDL1 expression in breast cancer. *Oncotarget*. 2015; 6(7):5449–5464. [PubMed: 25669979]

Translational Relevance

Identification of targeted therapies that activate anti-tumor immunity could offer a significant advance for cancer patients. PI3K inhibitors when combined with other targeted therapies have shown promise for treatment of breast and other cancers. Here we show that in addition to enhancing tumor growth and metastasis, activation of the PI3K pathway in immune cells suppresses anti-tumor immunity in mouse models of breast cancer. Moreover, combining pan-PI3K inhibition with immune check point blockade improves the therapeutic response by targeting both the tumor and its microenvironment. Our data indicate that clinical trials combining inhibitors of PI3K with anti-PD1 should be considered for triple negative breast cancers.

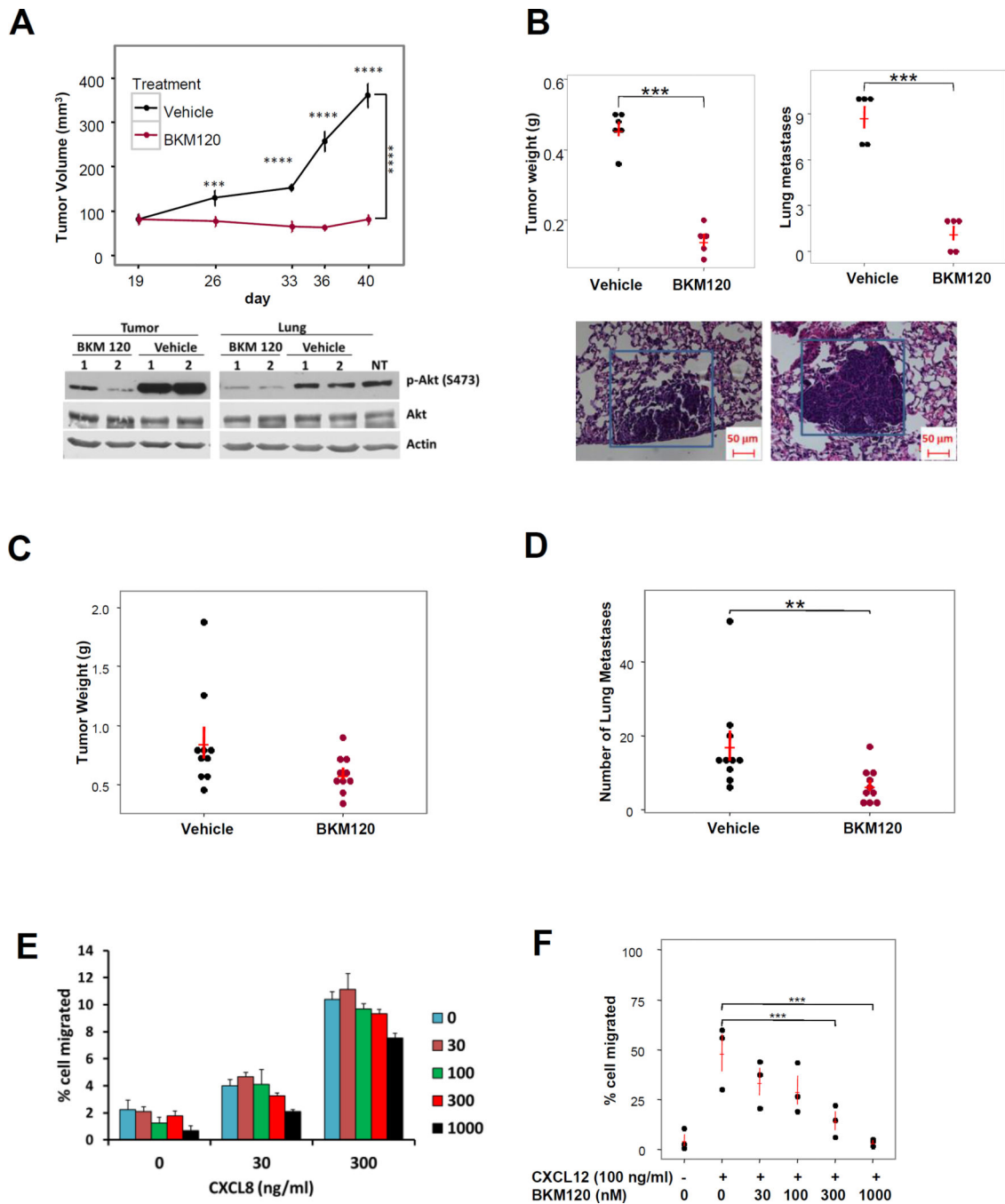


Figure 1. MMTV-PyMT and 4T1 tumor growth and metastasis are reduced in mice treated with the pan PI3K inhibitor BKM120

2×10^6 MMTV-PyMT mammary tumor cells were implanted into the fourth mammary fat pad of female C57Bl/6 mice. When tumors reached 60 mm^3 , mice were treated with BKM120 (30 mg/Kg, QD) or vehicle control ($n = 4-5$ mice per group). (A) Tumor growth was followed over 40 days ($p < 0.0001$, mixed-effects model with mean contrasts on a nature log scale; day 26 $p = 0.0001$, days 33, 36 and 40 $p < 0.0001$) and inhibition of Akt activation by BKM120 in tumors and lungs was confirmed by Western blots; (B) Tumor weight and number of lung metastases were evaluated after 40 days treatment by analysis of H&E

stained sections of perfused and fixed lungs (two sample t-test, $p < 0.0001$); (C) and (D) Nine-week old female BALB/c mice were implanted with 5×10^5 4T1 breast cancer cells. After 10 days when the tumors were palpable, mice were given vehicle control ($n = 10$) or 30 mg/kg BKM120 ($n = 10$) daily by oral gavage for 3 weeks. At the end of experiment, the mice were sacrificed, tumor volume was determined and lungs were processed for H&E staining and the number of metastases was determined by manual counting. Number of lung metastases are significantly higher in Vehicle group than in BKM120 group ($p=0.0035$, two sample t test on a log₂ scale), but not for tumor weight ($p=0.06$, two sample t test on a log₂ scale) E) BKM120 (0, 30, 100, 300, or 1000 nM) failed to inhibit chemotaxis toward a CXCL8 gradient (0, 30, 300 ng/ml of CXCL8) in mouse bone marrow neutrophils in a modified Boyden chamber assay. F) BKM120 inhibited invasion of PyMT mammary tumor cells in response to CXCL12 (100 ng/ml) in Matrigel transwell migration assays (ANOVA with Dunnett's test). Unless otherwise noted, * $p < 0.05$, ** $p < 0.01$, *** $p < 0.001$, **** $p < 0.0001$.

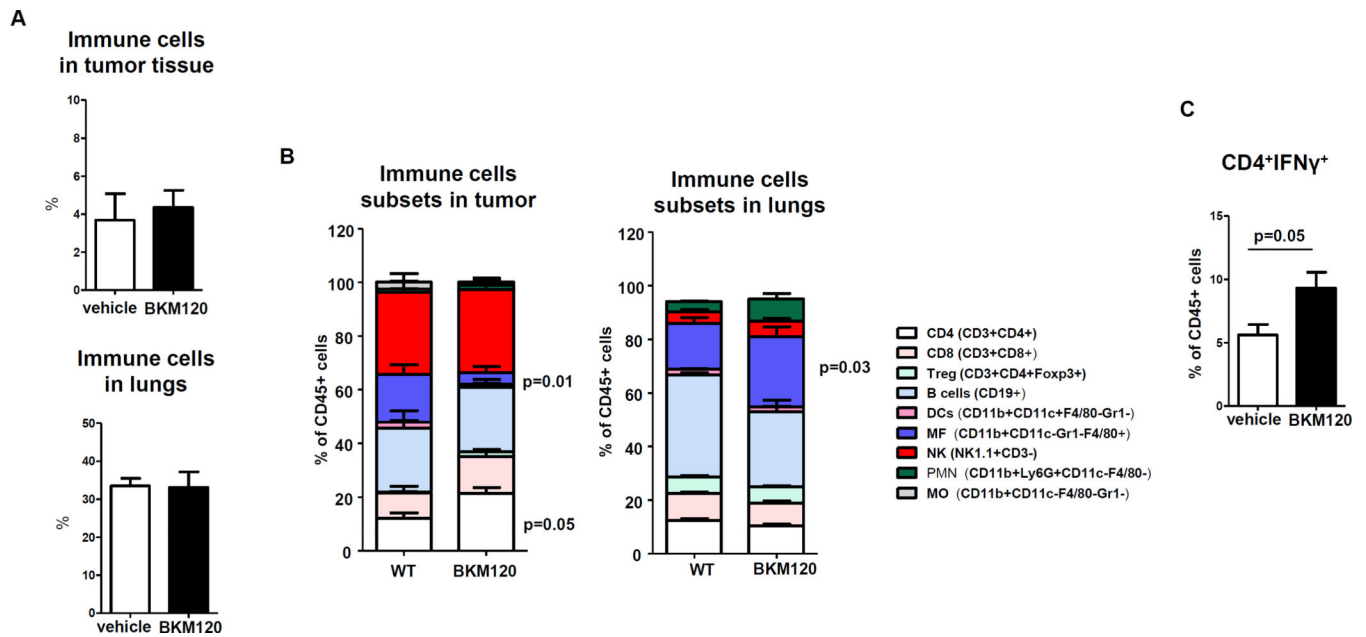


Figure 2. Type 1 T cell populations are increased in both tumor and lung of BKM120-treated mice bearing PyMT tumor 5 weeks after tumor cell implantation

((A) Compared to the vehicle control group, there was no change in the overall number of immune cells in the tumor or the lung after BKM120 treatment for 5 weeks. (B) Number of different subsets of immune cells in tumor tissue (left) and lungs (right) in % of immune cells (CD45) in mice treated with BKM120 vs. vehicle based on FACS analysis. (C) Number of CD4+IFN γ ⁺ cells based on intracellular analysis via FACS in BKM120 treated mice vs. vehicle. Group comparisons were made using Wilcoxon rank sum test.

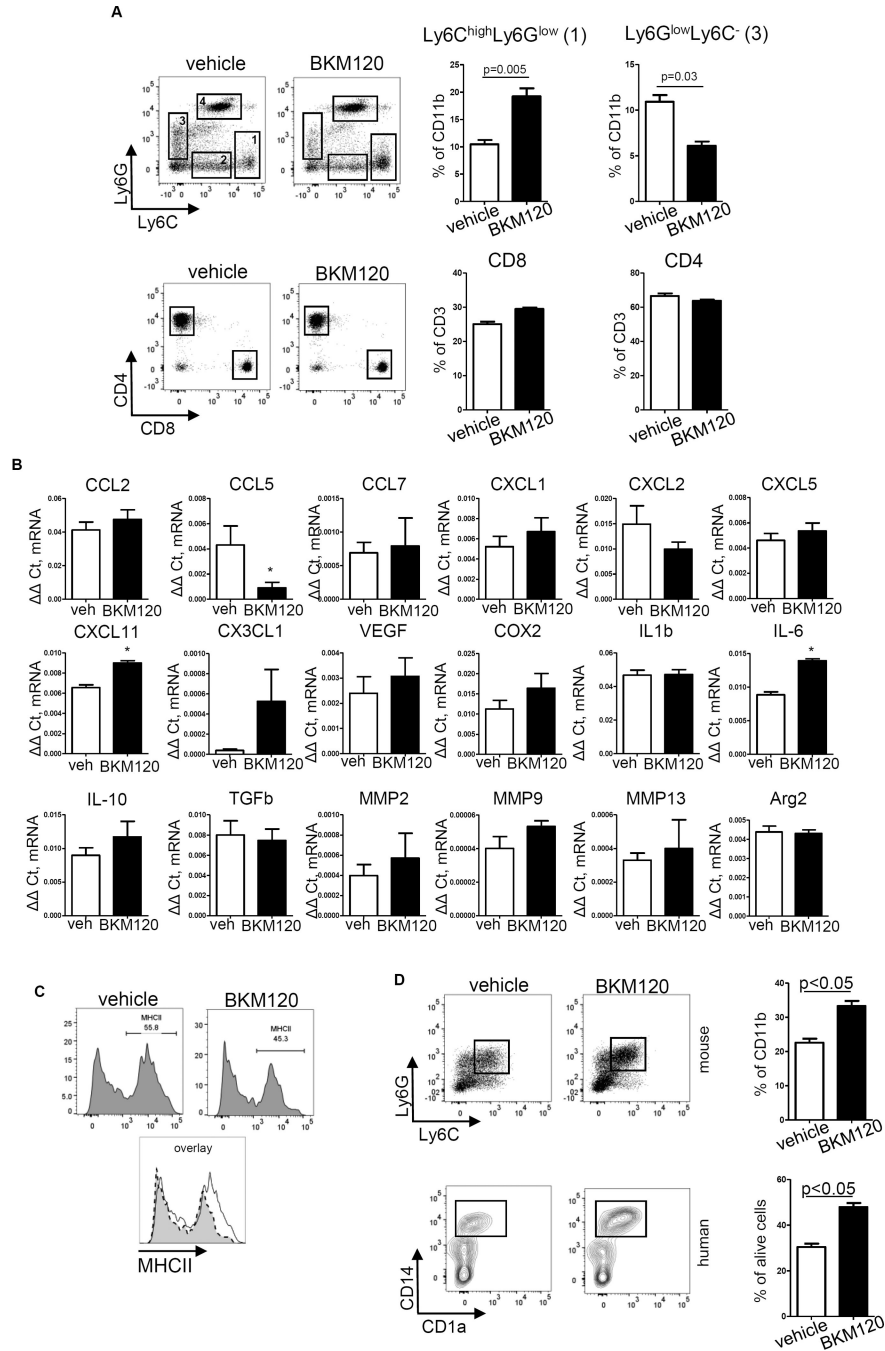


Figure 3. Increased accumulation of Ly6C⁺ leukocytes in lungs in mice pretreated with BKM120 (A) Significantly increased lung accumulation of CD11b⁺Ly6C⁺Ly6G^{low} leukocytes in the mice pretreated with BKM120. Non-tumor bearing BALB/c mice (9 week-old females) were treated with vehicle or BKM120 (30 mg/kg, daily) for two weeks, mice were sacrificed then single cell suspensions were generated from lungs and FACS analysis was performed. Plots are gated for CD45⁺CD11b⁺ cells. No differences were found in T cell number (plots are gated for CD45⁺CD3⁺ cells). (B) Gene expression profile (quantitative real-time PCR) FACS sorted CD11b⁺Ly6C⁺Ly6G^{low} leukocytes from lung of mice treated with BKM120 as

described above in A, * indicates $p < 0.05$. (C) MHCII expression on $CD11b^+Ly6C^+Ly6G^{low}$ leukocytes in lungs. (D) The *in vitro* differentiation of myeloid cells from mouse bone marrow (top) and human bone marrow (bottom) in presence of GM-CSF, 20 ng/ml and BKM120, 300 nM.

Author Manuscript

Author Manuscript

Author Manuscript

Author Manuscript

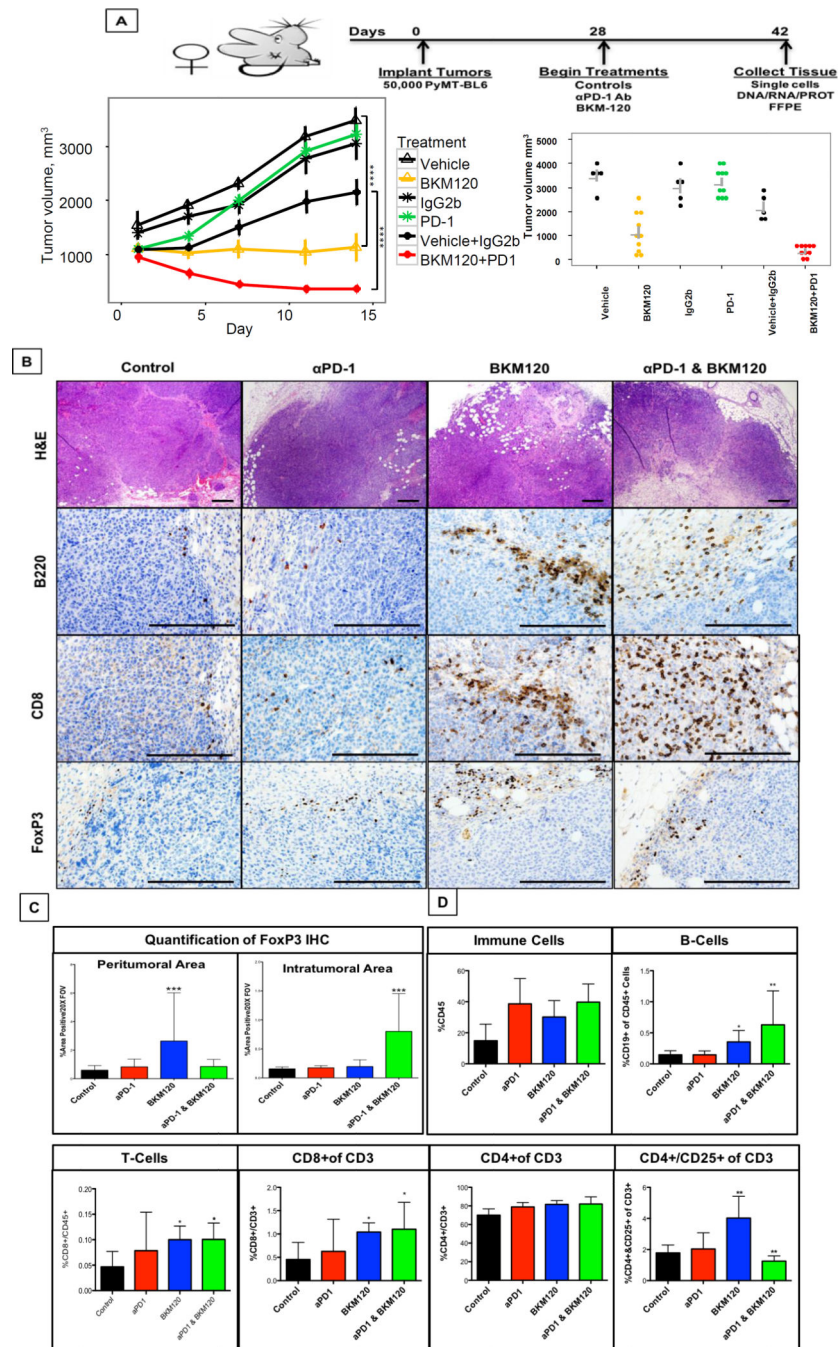


Figure 4. BKM120 is enhanced with combined anti-PD-1 immunotherapy

A) Eight week C57Bl/6 female non-parous mice were implanted orthotopically into the #4 mammary gland with 5.0×10^5 syngeneic PyMT cells. After 4 weeks when tumors reached a 1cm diameter, mice were treated with either a PD-1 blocking antibody (100ug twice a week), BKM120 (30mg/kg daily) or a combination of both αPD-1 and BKM120, for two weeks and then euthanized. There were 3 groups of control mice: 5 received DMSO (the solvent for the BKM120); 5 received a non-specific IgG (control for the anti-PD1); and 5 received a combination of both (control for anti-PD1 and BKM120 treatments). Left panel:

mean (s.e.) tumor volume over time. Measurements of tumor volume over time revealed significant reduction in growth with BKM120 treatment alone (adj. $p < 0.001$), while the tumors treated with the combination of BKM120 and anti-PD1 showed significantly greater reduction in growth and even regression [(adj. $p < 0.001$) ($n=10$), p -values from mixed-effects model, adjusted for multiplicity using the Benjamini & Hochberg method]. Right panel: average tumor volume (s.e.) at the 14th day. Differences in average tumor volume between BKM120+anti-PD1 and BKM120 were statistically significantly (adj. $p < 0.011$), while differences for each in comparison to vehicle control or vehicle plus IgG2b were also statistically significant ($p < 0.001$). p -values were determined by ANOVA. B) Histology of primary tumors typifies PyMT tumors as advanced adenocarcinomas with enhanced presence of B-cells, CD8 T-cells and FoxP3+ cells in BKM120 and combined treated tumors. C) Quantification of FoxP3 immunohistochemistry for both peri-tumoral area and intratumoral area revealed distinct accumulation of FoxP3+ cells in BKM120 (20x Field of View) compared with combined treatment. D) FACS analysis of immune cells from primary tumors increased leukocytes in α PD-1, BKM-120 or combined treatments, with significant increases in B-cells, T-cells and CD4+/CD25+ cells in BKM120 alone treated tumors, which was reversed with addition of α PD-1 combination. Error bars indicate SD and p -values were determined by one-way ANOVA. * $p < 0.05$ and *** $p < 0.001$. Scale bars in histology indicate 100 μ M.

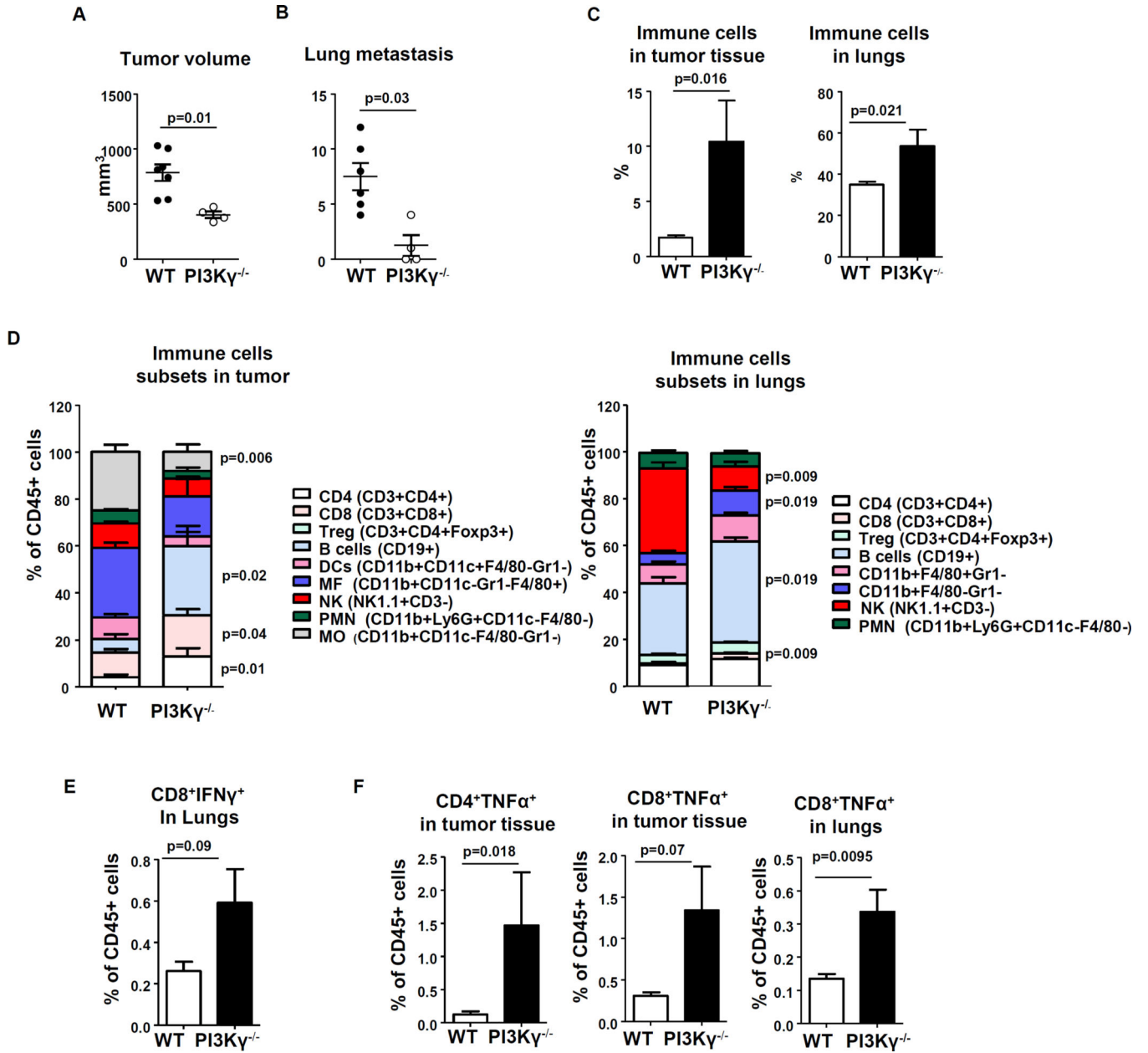


Figure 5. MMTV-PyMT murine mammary tumor growth and metastasis are inhibited in PI3K γ ^{-/-} mice

3x10⁶ MMTV-PyMT mammary tumor cells were implanted into the fourth mammary fat pad of PI3K γ ^{-/-} (n = 4) and WT C57BL/6 mice (n = 6) and tumor growth was monitored for 5 weeks after tumor cell implantation. (A) Final tumor volume was determined by fluid displacement. (B) Number of lung metastases were counted from H&E stained sections of paraformaldehyde-fixed paraffin-embedded tissue of each perfused lung. (C) Number of immune cells (CD45⁺) in tumor tissue and lungs by FACS analysis. (D) Immune cell subsets in tumor tissue (left) and in lungs (right) by FACS analysis. All cell population calculated as % of immune (CD45⁺) cells. (E) Number of IFN γ ⁺ CD8 cells in lungs and (F) number of TNF α ⁺ CD8 and CD4 cells in tumor tissue and lungs. Number of cells was calculated by

intracellular staining of a single cell suspension of tissue as described in M&M section.
Statistics: two sample t-test.

Author Manuscript

Author Manuscript

Author Manuscript

Author Manuscript

